Noname manuscript No.
(will be inserted by the editor)

Comparison of Deconvolution Algorithms of Phased Microphone Array for Sound Source Localization in an Airframe Noise Test

Jiayu Wang · Wei Ma

Received: date / Accepted: date

Abstract Nowadays phased microphone arrays have become a standard technique for acoustic source localization. The conventional beamforming constructs a dirty map of source distributions from array microphone pressure signals. Conventional beamforming is simple and robust, however its main disadvantages include poor spatial resolution particularly at low frequencies and poor dynamic range due to side-lobe effects. Deconvolution algorithms reconstruct a clean map of source distributions from a dirty map via iterative deconvolution, and thus can significantly improve the spatial resolution. Many deconvolution algorithms that have developed in many fields of imaging, such as optical and radio astronomy or optical microscopy, have gradually applied in acoustic-array measurements. The performances of these deconvolution algorithms have been compared using simulated applications and experimental applications with simple sound source distributions. However these comparisons are not carried out in experimental applications with complex sound source distributions. In this paper, the performances of five deconvolution algorithms (DAMAS, CLEAN-SC, NNLS, FISTA and SpaRSA) are compared in an airframe noise test, which contains very complex sound source distributions. DAMAS and CLEAN-SC achieve better spatial resolution than NNLS, FISTA and SpaRSA. DAMAS need more computational effort compared with CLEAN-SC. In addition, DAMAS can significantly reduce computational run time using compression computational grid. DAMAS with compression computational grid and CLEAN-SC are thus recommended for source localizations in experimental applications with complex sound distributions.

Keywords Microphone Array · Beamforming · Deconvolution Algorithms · Airframe Noise

✉Wei Ma E-mail: mawei@sjtu.edu.cn

Jiayu Wang · Wei Ma
School of Aeronautics and Astronautics, Shanghai Jiao Tong University,
Shanghai 200240, P. R. China

1 Introduction

Nowadays with the improvement of people's living standards, the demand for quiet and a comfortable environment is getting stronger and stronger. At the same time, the interest for acoustic source localization has been increasingly growing. Beamforming with arrays of microphones is indispensable for the localization of sound sources on moving objects, on flying aircraft, on high-speed trains, on motor cars in motion, on open rotors like helicopter and wind turbine rotors [1].

In order to better represent the distributed noise (such as the aerodynamic noise from the airframe) in microphone array measurements, the deconvolution algorithms are required. Deconvolution algorithms reconstruct a clean map of source distributions from a dirty map by iteratively deconvolution, and thus can significantly improve the spatial resolution [2–5].

For that purpose, a variety of deconvolution algorithms have been developed in the last several decades. In 1974, the non-negative least-squares (NNLS) was introduced by Lawson and Hanson [6], where all calculations are accelerated by spectral procedures. In 1998, Dougherty and Stoker [7] first applied CLEAN algorithm in sound source localization. Sijtsma [8] extended CLEAN to CLEAN-SC, which based on spatial source coherence. Unlike other deconvolution algorithms, it does not use the point spread function. It works well in combination with CSM (cross spectra matrix) diagonal removal [9]. At the 2004 AIAA/CEAS Aeroacoustic Conference, a breakthrough of deconvolution algorithms in acoustic microphone array technology was reported by Brooks and Humphreys, they applied DAMAS algorithm in acoustic array measurements [10, 11]. Between 2005 and 2006, Brooks and Humphreys extended it to three-dimensional acoustic image [12] and for coherent acoustic sources [13]. Unfortunately, DAMAS usually requires high computational effort in most situations. In 2017, Ma and Liu [14–16] published their work on compression computational grid, where they can successfully improve the efficiency of DAMAS via compression computational grid that only contains the significant grid points and does not contain the redundant grid points.

On many occasions, it has turned out that it is necessary to have a better assessment of these deconvolution algorithms using a set of common data sets. Many researchers have drawn the attention of the comparison of these deconvolution algorithms using simulated applications and experimental applications with simple sound source distributions. Ehrenfried et al. [17] have applied the three deconvolution algorithms DAMAS2 [18], the Fourier-based NNLS and Richardson-Lucy (RL) [19, 20] to reconstruct the source distributions from the dirty map with a line array and a one-dimensional region of interest. Herold et al. [21] compared several deconvolution algorithms using data from an aeroacoustic measurement of NACA 0012 airfoil positioned in an open jet. Recently, Bahr et al. [22] compared several common microphone phased array processing techniques applied to two open datasets. However the comparison of DAMAS, CLEAN-SC, NNLS, FISTA and SpaRSA haven't been

carried out in experimental applications with complex sound source distributions.

The main purpose of this paper is to determine which deconvolution algorithms (DAMAS, CLEAN-SC, NNLS, FISTA and SpaRSA) can play a better role for source localization in experimental applications with complex sound distributions. The benchmark test DLR1 is used to assess these deconvolution algorithms. The DLR1 benchmark test consists of a test configuration with a Dornier-728 semispan (or half) model in the high-lift configuration in the cryogenic wind tunnel at the DLR Cologne site (Kryo-Kanal Koeln, DNW-KKK) [23]. One goal is to carry out the application of several deconvolution algorithms in aeroacoustic measurements. Another objective is to carry out the comparison of these deconvolution algorithms.

The rest of this paper is organized as follows. Conventional beamforming and deconvolution algorithms are illustrated in Section 2. Experimental applications with complex source distributions are carried out in Section 3. A discussion is given in Section 4. Finally, conclusions are presented in Section 5.

2 Conventional beamforming and deconvolution algorithms

Conventional beamforming is simple and robust. Conventional beamforming can construct a dirty map of source distributions from array microphone pressure signals. However its main disadvantages include poor spatial resolution particularly at low frequencies and poor dynamic range due to side-lobe effects.

Brooks and Humphrey [10, 11] proposed DAMAS algorithm, which is an iterative algebraic deconvolution algorithm. DAMAS aims at solving the convolution equation by a Gauss-Seidel procedure, replacing nonphysical negative solutions by zero and achieving more accurately quantify position and strength of acoustic sources.

In order to remove side lobes actually measured beam patterns. Sijtsma [8] launched CLEAN-SC. CLEAN-SC can successfully extract absolute sound power levels from the source plots [8]. CLEAN-SC basically performs a decomposition of the CSM into coherent components. Unlike other deconvolution algorithms, it does not use the point spread function. It works well in combination with CSM diagonal removal.

NNLS [6] algorithm aims directly at the minimization of the square sum of the residuals. A gradient-type procedure is used to solve the NNLS problem.

FISTA [24] deconvolution algorithm is ideally suitable for image reconstruction from indirect and possibly under-sampled data and can achieve high computational simplicity.

Sparse Reconstruction by Separable Approximation (SpaRSA) is an iterative deconvolution algorithm to a minimum of the objective function and suitable for solving large-scale optimization problems involving the sum of a smooth error term and a possibly non-smooth regularizer [25]. SpaRSA has

far-reaching effects in the field of imaging. More details for SpaRSA can be found in [25].

3 Experimental applications

In this section, five different deconvolution algorithms (DAMAS, CLEAN-SC, NNLS, FISTA and SpaRSA) are applied to benchmark test DLR1. This acoustic-array measurement [23] performed in a cryogenic wind tunnel at the DLR Cologne site, Kryo-Kanal Koeln (DNW-KKK) using a 9.24% Dornier 728 half-model. This cryogenic wind tunnel is a continuous-flow low-speed wind tunnel (DNW-KKK) with a 2.4×2.4 m closed-wall test section. By injection of liquid nitrogen, This wind tunnel can be operated in the range of $100 < T < 300$K at Mach number up to 0.38. Fig. 1 indicates the test setup. A spiral microphone array consisting of 144 microphones is designed and constructed for this measurement. The array is mounted by the compressed laminated wood onto the sidewall, and the Dornier 728 half-model is located in the center of the test section. The model of scale 1:9.24 is configured in a landing configuration and has a mean aerodynamic chord length of 0.353m and a half-span width of 1.44m. More details for this measurement can be found in [23]. Recently, a comparison of microphone phased array methods applied to the benchmark test DLR1 was carried out by Bahr et al. [22].

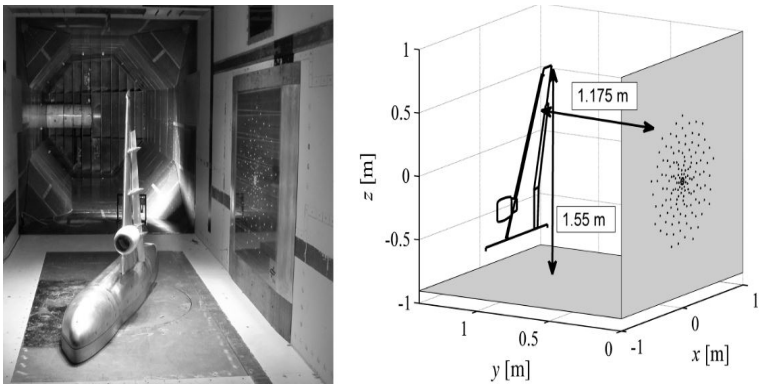

Fig. 1 Photo of the test section with the array mounted on the side wall (left) and the Dornier 728 half-model in the center, view in flow direction. Drawing of the measurement setup (right) [23].

The data processing is carried out on an Intel Core i5-4210H 2.90GHz processor with MATLAB. The information of this data processing is listed in Table 1. The choice of angle of attack, Mach number, temperature and plotting scale is for the sake of comparison with the deconvolution result of Bahr et al. [22]. The computational grid used in this paper is the same as that in the benchmark. The rotation of the computational grid is the same

as that introduced in Bahr et al. [22]. In the calculation of the dirty map of conventional beamforming, CSM is directly from the benchmark test data. In the process of calculating the steering vector, the influence of Mach number is taken into account. There are two different experimental applications, in which frequencies are $f = 8496$Hz and $f = 6300$Hz, respectively, plotted in Fig. 2 and 3. The computational run time of these experimental applications is listed in Table 2.

3.1 Spatial resolution

3.1.1 Case 1, $f = 8496Hz$

The deconvolution results of $f = 8496$Hz case is very similar to the recent deconvolution results of Bahr et al. [22].

The dirty map of conventional beamforming shown by Fig. 2(a) is quite similar to the source maps of conventional beamforming contributed by DLR has shown in Fig. 4(a) in [22]. There are two main noise sources when $f = 8496$Hz. One is the slat noise near the leading edge. The other one is the flap side edge noise.

Fig. 2(b) indicates the clean map of DAMAS on original grid which is very similar to the DAMAS result contributed by DLR in Fig. 5(h) in [22]. The slat noise and the flap noise are well distributed in this clean map, due to significantly improved spatial resolution.

The clean map of CLEAN-SC shown in Fig. 2(c) is also quite similar to the CLEAN-SC result contributed by DLR in Fig. 4(c) in [22]. This clean map can achieve high spatial resolution containing exactly one source on every slat and one source on the flap side edge.

In Fig. 2(d), Fig. 2(e) and Fig. 2(f), NNLS, FISTA and SpaRSA are applied to the benchmark DLR1 that shows only slightly fewer sources. However, the peak level is nearly as same as the result of DAMAS and CLEAN-SC.

Compared with Fig. 2(a), the clean map of DAMAS with compression computational grid based on conventional beamforming (denoted by DAMAS-CG2 [14]) shown in Fig. 2(g) can retain the spatial resolution of DAMAS on original grid.

3.1.2 Case 2, $f = 6300Hz$

In order to carry out this comparison in different frequencies, in the second application frequency is set as 6300Hz. In this case, there is only one high region dominated the dirty map of conventional beamforming. That is the slat noise near the leading edge. As shown in Fig. 3(b), Fig. 3(c) and Fig. 3(g), DAMAS, CLEAN-SC and DAMAS-CG2 can identify separately most slat noise sources. Fig. 3(d), Fig. 3(e) and Fig. 3(f) show the deconvoluted results of NNLS, FISTA and SpaRSA. The spatial resolutions are a little slighter than that of DAMAS, CLEAN-SC and DAMAS-CG2.

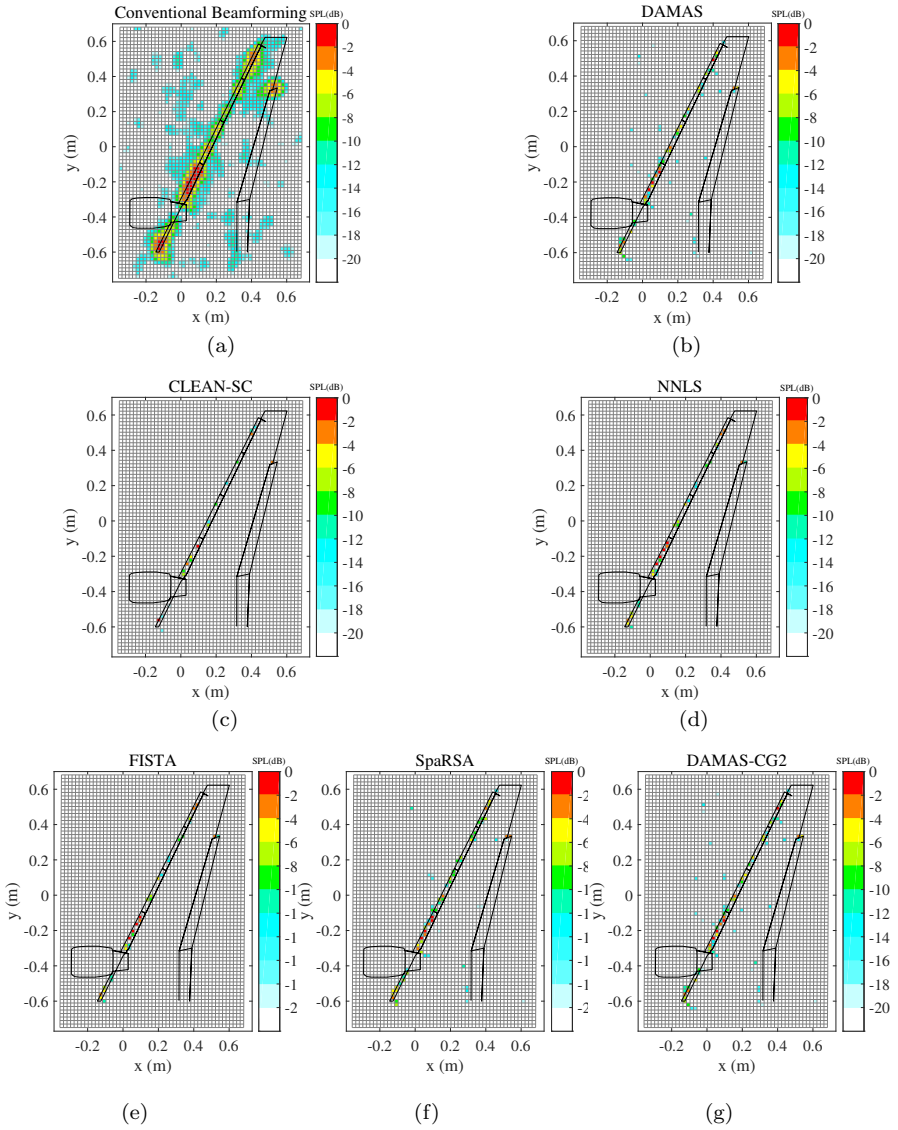

Fig. 2 Sound pressure level maps of Benchmark test DLR1. $f = 8496$Hz. The location of the Dornier 728 half-model is sketched in the background. (a) Dirty map of conventional beamforming. (b)Deconvolved map of DAMAS on original grid. (c) Deconvolved map of CLEAN-SC. (d) Deconvolved map of NNLS. (e) Deconvolved map of FISTA.(f) Deconvolved map of SpaRSA. (g) Deconvolved map of DAMAS on compression grid.

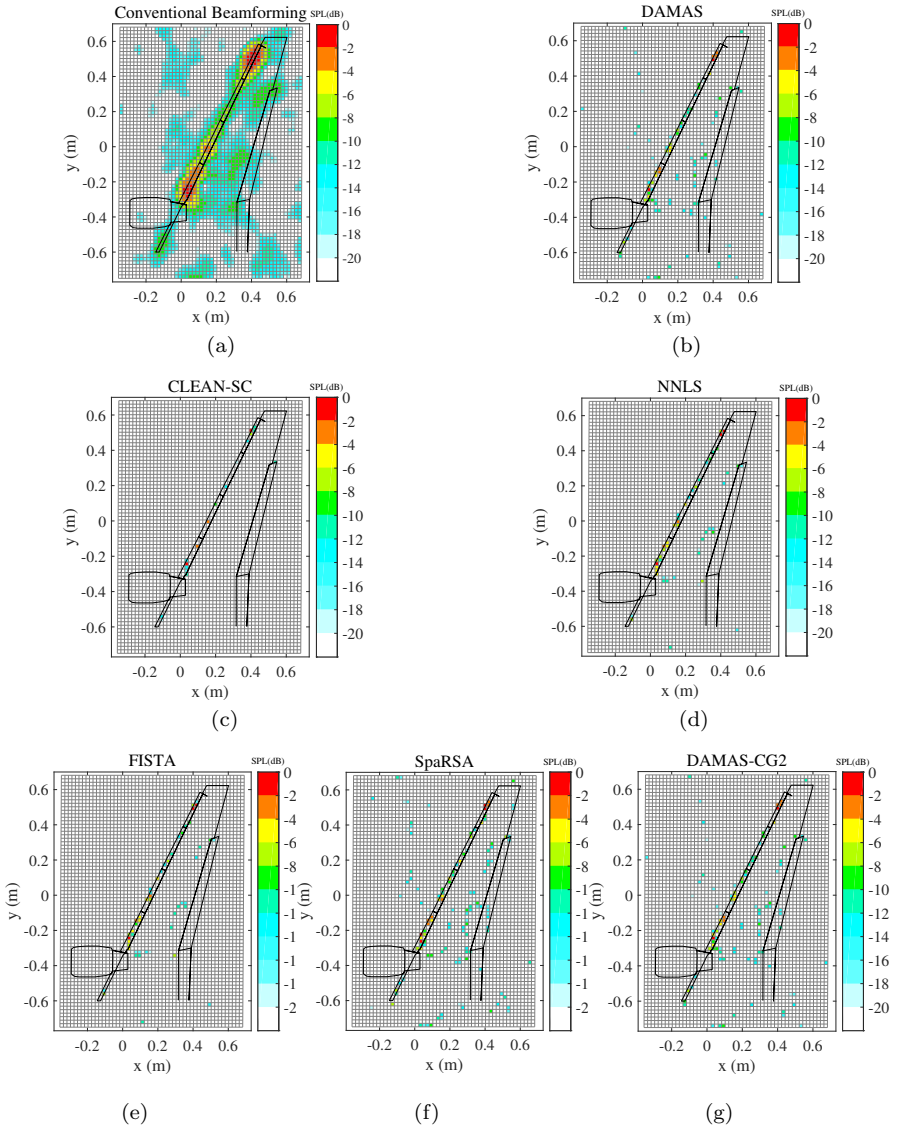

Fig. 3 Sound pressure level maps of Benchmark test DLR1. $f = 6300$Hz The location of the Dornier 728 half-model is sketched in the background. (a) Dirty map of conventional beamforming. (b)Deconvolved map of DAMAS on original grid. (c) Deconvolved map of CLEAN-SC. (d) Deconvolved map of NNLS. (e) Deconvolved map of FISTA.(f) Deconvolved map of SpaRSA. (g) Deconvolved map of DAMAS on compression grid.

Table 1 Information of data processing

Angle of attack	3°
Mach number	0.25
Temperature	290K
Grid resolution	20mm
The computational grid	53×73 with 3869 points in x-y plane
Plotting scale	20dB
Number of iterations	2000

Table 2 Computational run time of different deconvolution algorithms

Deconvolution algorithms	Computational run time	
	Case 1	Case 2
DAMAS	1416s	1623s
CLEAN-SC	51s	33s
NNLS	1255s	1456s
FISTA	1264s	1470s
SpaRSA	1370s	1790s
DAMAS-CG2	237s	501s

3.2 Computational run time

The computational run time of different deconvolution algorithms in Case 1 and Case 2 is shown in Table 2. The computational efficiency of CLEAN-SC is obvious in both two cases.

In Case 1, the computational run time of DAMAS, NNLS, FISTA and SpaRSA are 1416s, 1255s, 1264s and 1370s, respectively, while that of CLEAN-SC is only 51s.

In Case 2, the computational run time of DAMAS, NNLS, FISTA and SpaRSA are 1623s, 1456s, 1470s and 1790s, respectively, while that of CLEAN-SC is only 33s.

DAMAS-CG2 can successfully reduce computational run time. The computer run time of DAMAS-CG2 in both two cases are only 237s and 501s, respectively.

4 Discussion

In this paper in order to compare the performance of five different deconvolution algorithms (DAMAS, CLEAN-SC, NNLS, FISTA and SpaRSA) in experimental applications with complex sound distributions, we apply these deconvolution algorithms to the benchmark DLR1.

The following statements are only valid for the angle of attack $\alpha = 3°$, $Ma = 0.25$, $T = 290$K, $f = 8496$Hz & $f = 6300$Hz, the grid resolution $d_{xy} = 20$mm and plotting scale 20dB.

When applied to aeroacoustic measurements with complex sound source distributions, these deconvolution algorithms are observed to behave as follows:

- **Conventional Beamforming**
  The result of conventional beamforming is a dirty map and all sound sources are visible. However it has poor spatial resolution and side-lobe effects.
- **DAMAS and CLEAN-SC**
  DAMAS and CLEAN-SC can significantly improve spatial resolution. Noise sources can be well distributed.
- **NNLS, FISTA and SpaRSA**
  NNLS, FISTA and SpaRSA can only distinguish slightly fewer source.
- **Computational Efficiency**
  CLEAN-SC is much faster than DAMAS, NNLS, FISTA and SpaRSA. However, DAMAS-CG2 can achieve similar spatial resolution with DAMAS. The computational run time of DAMAS-CG2 is longer than CLEAN-SC. While compared with other three deconvolution algorithms, DAMAS-CG2 can greatly reduce the computational run time.

5 Conclusion

Five different deconvolution algorithms (DAMAS, CLEAN-SC, NNLS, FISTA and SpaRSA) are compared through applications to the benchmark DLR1. The spatial resolution and computational run time are selected as the main criteria in this comparison.

In terms of spatial resolution, every deconvolution algorithms described above can distribute the dominant sound source. DAMSA and CLEAN-SC can successfully improve the spatial resolution and achieve higher spatial resolution than NNLS, FISTA and SpaRSA.

In terms of computational run time, CLEAN-SC is much faster than the other four deconvolution algorithms described above. DAMAS with compression computational grid can significantly reduce computational run time.

In order to obtain higher spatial resolution and greatly improve the computational efficiency, DAMAS with compression computational grid and CLEAN-SC are thus recommended for source localization in experimental applications with complex sound distributions. For the future investigations, it will be of interest to improve the computational efficiency of NNLS, FISTA and SpaRSA.

Acknowledgements This work is under the generous support of School of Aeronautics and Astronautics in Shanghai Jiao Tong University.

References

1. U. Michel, History of acoustic beamforming, in: Proceedings of 1st Berlin Beamforming Conference, 2006.

2. B. R. Frieden, Restoring with maximum likelihood and maximum entropy, Journal of the Optical Society of America 62 (4) (1972) 511–518.
3. M. R. Banham, A. K. Katsaggelos, Digital image restoration, IEEE Signal Processing Magazine 14 (2) (1977) 24–41.
4. S. F. Gull, G. J. Daniell, Image reconstruction from incomplete and noisy data, Nature 272 (5655) (1978) 686–690.
5. R. Narayan, R. Nityananda, Maximum entropy image restoration in astronomy, Annual Review of Astronomy & Astrophysics 24 (1) (1986) 127–170.
6. C. L. Lawson, R. J. Hanson, Solving least squares problems, Mathematics of Computation 30 (135) (1995) 665.
7. R. P. Dougherty, R. W. Stoker, Sidelobe suppression for phased array aeroacoustic measurements, in: 4th AIAA/CEAS Aeroacoustics Conference, 1998.
8. P. Sijtsma, CLEAN based on spatial source coherence, International Journal of Aeroacoustics 6 (4) (2009) 357–374.
9. E. Sarradj, G. Herold, P. Sijtsma, R. Merino Martinez, T. F. Geyer, C. J. Bahr, R. Porteous, D. Moreau, C. J. Doolan, A microphone array method benchmarking exercise using synthesized input data, in: 23rd AIAA/CEAS Aeroacoustics Conference, 2017.
10. T. F. Brooks, W. M. Humphreys, A deconvolution approach for the mapping of acoustic sources (DAMAS) determined from phased microphone arrays, in: 10th AIAA/CEAS Aeroacoustics Conference, 2004.
11. T. F. Brooks, W. M. Humphreys, A deconvolution approach for the mapping of acoustic sources (DAMAS) determined from phased microphone arrays, Journal of Sound & Vibration 294 (4) (2006) 856–879.
12. T. F. Brooks, W. M. Humphreys, Three-dimensional applications of DAMAS methodology for aeroacoustic noise source definition, in: 11th AIAA/CEAS Aeroacoustics Conference, 2005.
13. T. F. Brooks, W. M. Humphreys, Extension of damas phased array processing for spatial coherence determination (DAMAS-C), in: 12th AIAA/CEAS Aeroacoustics Conferences, 2006.
14. W. Ma, X. Liu, DAMAS with compression computational grid for acoustic source mapping, Journal of Sound & Vibration 410 (2017) 473–484.
15. W. Ma, X. Liu, Improving the efficiency of DAMAS for sound source localization via wavelet compression computational grid, Journal of Sound & Vibration 395 (2017) 341–353.
16. W. Ma, X. Liu, Compression computational grid based on functional beamforming for acoustic source localization, Applied Acoustics 134 (2018) 75 – 87.
17. K. Ehrenfried, L. Koop, Comparison of iterative deconvolution algorithms for the mapping of acoustic sources, AIAA Journal 45 (7) (2007) 1–19.
18. R. P. Dougherty, Extensions of DAMAS and benefits and limitations of deconvolution in beamforming, in: 11th AIAA/CEAS Aeroacoustics Conference, 2013.
19. L. B. Lucy, An iterative technique for the rectification of observed distributions, The Astronomy Journal 79 (6) (1974) 745–754.
20. W. H. Richardson, Bayesian-based iterative method of image restoration, Journal of the Optical Society of America 62 (1) (1972) 55–59.
21. G. Herold, T. F. Geyer, E. Sarradj, Comparison of inverse deconvolution algorithms for high-resolution aeroacoustic source characterization, in: 23rd AIAA/CEAS Aeroacoustics Conference, 2017.
22. C. J. Bahr, W. M. Humphreys, D. Ernst, T. Ahlefeldt, C. Spehr, A. Pereira, Q. Leclre, C. Picard, R. Porteous, D. Moreau, J. R. Fischer, C. J. Doolan, A comparison of microphone phased array methods applied to the study of airframe noise in wind tunnel testing, in: 23rd AIAA/CEAS Aeroacoustics Conference, 2017.
23. T. Ahlefeldt, Aeroacoustic measurements of a scaled half-model at high reynolds numbers, AIAA Journal 51 (12) (2013) 2783–2791.
24. A. Beck, M. Teboulle, A fast iterative shrinkage-thresholding algorithm for linear inverse problems, SIAM Journal on Imaging Sciences 2 (1) (2009) 183–202.
25. S. J. Wright, R. D. Nowak, M. A. T. Figueiredo, Sparse reconstruction by separable approximation, IEEE Transactions on Signal Processing 57 (7) (2009) 2479–2493.